JACS
JOURNAL OF THE AMERICAN CHEMICAL SOCIETY

Article

pubs.acs.org/JACS

Probing Structure and Function of Ion Channels Using Limited Proteolysis and Microfluidics

Carolina L. Trkulja,[†] Erik T. Jansson,[†,‡] Kent Jardemark,[†,§] and Owe Orwar*[,∥]

[†]Department of Chemical and Biological Engineering, Chalmers University of Technology, SE-412 96 Göteborg, Sweden
[∥]Department of Physiology and Pharmacology, Karolinska Institutet, SE-171 77 Stockholm, Sweden

Supporting Information

ABSTRACT: Even though gain, loss, or modulation of ion channel function is implicated in many diseases, both rare and common, the development of new pharmaceuticals targeting this class has been disappointing, where it has been a major problem to obtain correlated structural and functional information. Here, we present a microfluidic method in which the ion channel TRPV1, contained in proteoliposomes or in excised patches, was exposed to limited trypsin proteolysis. Cleaved-off peptides were identified by MS, and electrophysiological properties were recorded by patch clamp. Thus, the structure–function relationship was evaluated by correlating changes in function with removal of structural elements. Using this approach, we pinpointed regions of TRPV1 that affect channel properties upon their removal, causing changes in current amplitude, single-channel conductance, and EC_{50} value toward its agonist, capsaicin. We have provided a fast "shotgun" method for chemical truncation of a membrane protein, which allows for functional assessments of various peptide regions.

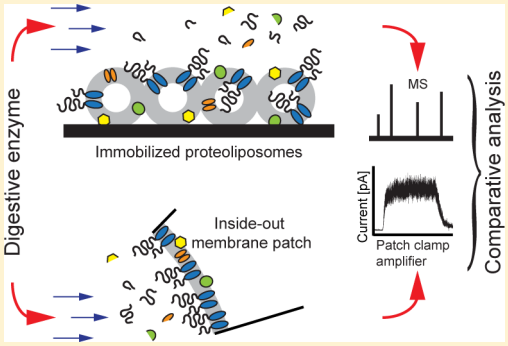

INTRODUCTION

There is an increasing demand for drugs targeting ion channels, given the severity and high unmet medical need in many indications where they play a key role, e.g., psychiatric and neurodegenerative disorders.[1,2] However, there has been few new drug registrations, and to a large part this is caused by the complexity of the diseases, as well as the inherent difficulty in studying ion channels. It is difficult to obtain structural data from ion channels with conventional techniques such as X-ray crystallography or NMR, due to their physicochemical properties, including the presence of several hydrophobic regions in the plasma membrane, their low natural abundance, and their instability to detergents.[3,4] Several researchers have, despite these difficulties, managed to demonstrate crystal structures of ion channels, e.g., Roderick MacKinnon and colleagues who presented the crystal structure of the KcsA potassium channel.[5] Correlation of structure and function of ion channels is commonly achieved with electrophysiological techniques while using genetically modified versions of the protein, e.g., site-directed mutagenesis of specific amino acids in the protein.[6−11] However, a major disadvantage of site-directed mutagenesis of ion channels is that the methodological procedures of generating and analyzing such mutant ion channels are time-consuming and laborious. Also, when designing the mutation, some pre-existing knowledge or hypothesis regarding the function of the chosen residue is required.[12] Thus, novel and efficient methodological approaches are needed for systematic evaluation of structure–function relationships for membrane proteins.

We have previously described a microfluidic flow cell that utilizes a lipid-based protein immobilization (LPI) technology, allowing direct chemical modulation of membrane proteins in their native lipid environment.[13] By deriving proteoliposomes from cells and immobilizing these into the flow cell, a stationary phase of membrane proteins is created which can be subjected to several rounds of solutions and different types of chemical modulations, e.g., by enzymes. Herein, we describe methods that use the LPI flow cell as a stand-alone device or in combination with an open-volume microfluidic flow cell for fast solution exchange suitable for patch-clamp experiments. The purpose is to obtain correlated structural and functional data using limited and controlled proteolysis of the ion channels, which is demonstrated in a schematic comparison of the two flow cells (Figure 1). It takes advantage of small-scale systems that allow for very fast transport times, whereby the environment surrounding the ion channels can be controlled exactly, and digestion times can be substantially shorter than in large-scale systems.[14] Whereas trypsin was utilized in the present study, it is important to note that other digestive enzymes can be used to optimize the protocol for a given application.

Here, we demonstrate this microfluidic approach of limited and controlled trypsin proteolysis, using the transient receptor potential vanilloid 1 (TRPV1) ion channel as a model protein. TRPV1 is a cation channel which is expressed in nociceptive

Received: July 24, 2014
Published: September 25, 2014

dx.doi.org/10.1021/ja507285w | J. Am. Chem. Soc. 2014, 136, 14875−14882

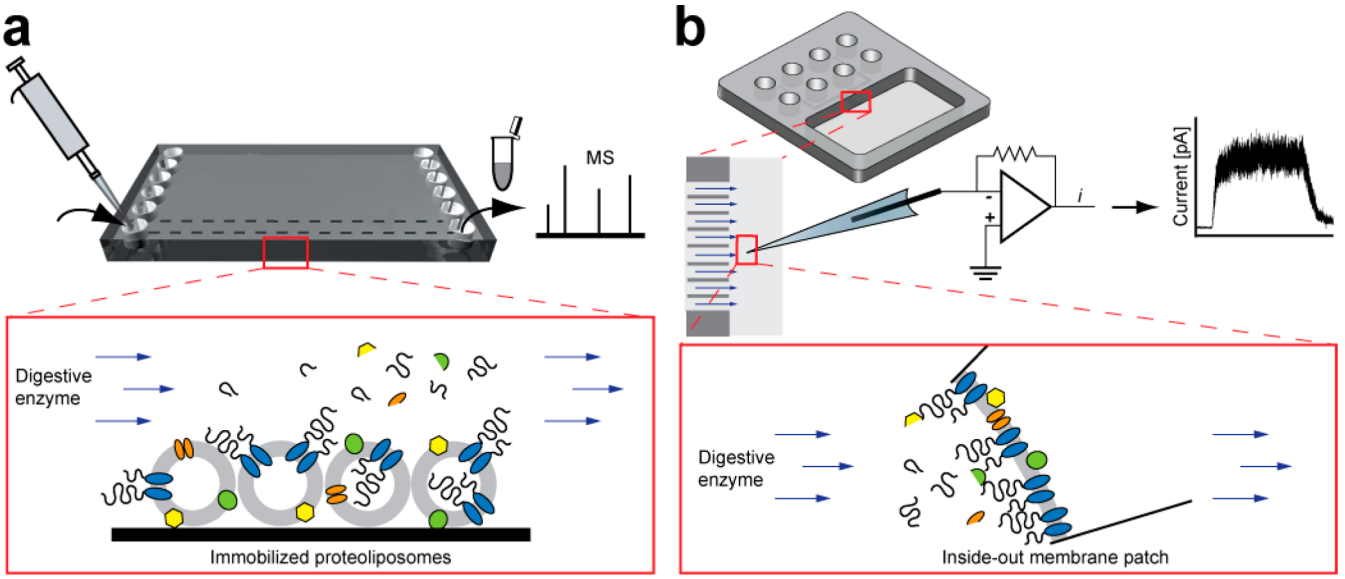

Figure 1. Comparison of the LPI and open-volume flow cells. (a) Schematic representation of the LPI flow cell. Here, proteoliposomes (diameter 50−150 nm) have been derived from cultured cells expressing the ion channel of interest and subsequently immobilized within the flow cell. This creates a stationary phase of membrane proteins that can be subjected to multiple rounds of solution without loss of material. When a digestive enzyme is injected into the flow cell, peptides are digested from the membrane proteins and can easily be eluted and identified with LC-MS/MS. (b) Schematic representation of the open-volume flow cell, suitable for patch-clamp experiments. Here we use an inside-out configuration, allowing the cytosolic side of an ion channel to be exposed to a digestive enzyme.

primary sensory neurons. This ion channel is responsible for pain sensation upon activation with, e.g., low pH, capsaicin, and several inflammatory mediators[8,15,16] and is considered an important drug target for pain relief.[17−20]

METHODS

Chemicals. Cell culturing medium (DMEM/Ham's F12 with glutamine), fetal bovine serum (FBS), and Accutase were purchased from PAA; Zeocin, Fura-2, and Calcium Sponge S were purchased from Invitrogen. Sequencing-grade modified trypsin was purchased from Promega. All other chemicals were purchased from Sigma. The following buffers were used: A, 300 mM NaCl, 10 mM Tris, pH 8.0; B, 300 mM NaCl, 10 mM Tris, 5 mM $CaCl_2$, pH 8.0; C, 300 mM NaCl, 10 mM Tris, 10 mM EGTA, pH 8.0; D, 140 mM NaCl, 5 mM KCl, 1 mM $MgCl_2$, 1 mM $CaCl_2$, 10 mM HEPES, 10 mM D-glucose, pH 7.4; E, 140 mM NaCl, 5 mM KCl, 1 mM $MgCl_2$, 10 mM HEPES, 10 mM D-glucose, 10 mM Na_4BAPTA, pH 7.4; F, 120 mM KCl, 2 mM $MgCl_2$, 10 mM HEPES, 10 mM K_4BAPTA, pH 7.2; G, 120 mM KCl, 2 mM $MgCl_2$, 10 mM HEPES, 10 mM K_4BAPTA, pH 8.0; H, 20 mM NH_4HCO_3, pH 8.0.

Cell Culture. Adherent Chinese hamster ovary (CHO) cells with a tetracycline-regulated expression system (T-REx) were cultivated in medium (DMEM/F12 with glutamine) supplemented with 10% FBS, Zeocin (350 μg/mL), and Blasticidin (5 μg/mL) in T175 or T500 culture flasks (Nunc) or on glass dishes. Before use (18−24 h), the cells were incubated in medium (DMEM/F12 with glutamine) supplemented with 10% FBS and Doxycycline (1 μg/mL) in order to induce expression of human TRPV1. The cell line was routinely tested for mycoplasma infection.

Proteoliposome Preparation. Proteoliposomes were prepared as previously described elsewhere[13] in either buffer A or B. Each proteoliposome preparation originated from several different culture flasks. Proteoliposomes loaded with 5 mM $CaCl_2$ (buffer B) were used for activity studies with Fura-2, whereas proteoliposomes without added Ca^{2+} (buffer A) were used for proteomic experiments.

TRPV1 Activity in Proteoliposomes. Proteoliposomes containing buffer B were immobilized inside the flow cell and washed with 1 mL of buffer A followed by 1 mL of buffer H. A 100 μL solution of 5 μg/mL trypsin in buffer H was injected into the channel and eluted with 100 μL of buffer H after 0.5 or 5 min. Before further use, buffer A was passed through a calcium sponge, in order to decrease calcium concentration to nanomolar levels, and thereafter stored in plastic tubes. After tryptic digestion, or immediately after proteoliposome immobilization in the case of naïve ion channels, external calcium was removed by washing the channel with 2 × 1 mL of buffer C followed by 1 mL of buffer A. A 100 μL solution of 5 μM Fura-2 in buffer A was injected into the flow cell, incubated for 1 min in room temperature for naïve ion channels and 5 min for digested ion channels in order to detect any calcium leakage after digestion, and then eluted with 100 μL of 5 μM Fura-2 in buffer A. Subsequently, 100 μL of 10 μM capsaicin and 5 μM Fura-2 in buffer A was injected into the flow cell, incubated for 5 min at room temperature, and then eluted with 100 μL of 10 μM capsaicin and 5 μM Fura-2 in buffer A. A Cary eclipse fluorescence spectrophotometer (Agilent Technologies, Santa Clara, CA, USA) was used to measure Fura-2 fluorescence. Fura-2 was excited between 250 and 450 nm, and fluorescence emission was measured at 510 nm. The ratio of the fluorescence intensities at 340 and 380 nm was used to calculate the calcium concentration in the samples. For determination of statistical significance between calcium release before and after treatment, Student's paired t test was applied, and $p < 0.05$ was considered as significant. Data are presented as mean ± 1 standard deviation.

Digestion Protocols. Sequential and single digestions within the flow cell were conducted as described elsewhere.[13] Limited proteolysis with different incubation times was performed in a sequential manner for 0.5, 5, 15, 30, 60, and 120 min. Trypsin was dissolved in buffer H. Eluted samples were digested overnight in Eppendorf tubes and analyzed with LC-MS/MS. Limited proteolysis in combination with electrophysiological recordings was performed with single digestions for 5 min with 5, 20, and 40 μg/mL trypsin dissolved in buffer G. Digestion was inhibited in some samples by addition of formic acid to a final concentration of 12%, whereas some eluents were digested overnight in Eppendorf tubes.

Liquid Chromatography with Tandem Mass Spectrometry. Peptide samples from digestions of CHO-proteoliposomes were analyzed at the Proteomics Core Facility at Gothenburg University, Göteborg, Sweden, as previously described.[13] All tandem mass spectra were searched by MASCOT (Matrix Science, London, UK) against UniProtKB release 2013_04 (Human, [*Homo sapiens*]; Swiss-Prot

dx.doi.org/10.1021/ja507285w | J. Am. Chem. Soc. 2014, 136, 14875−14882

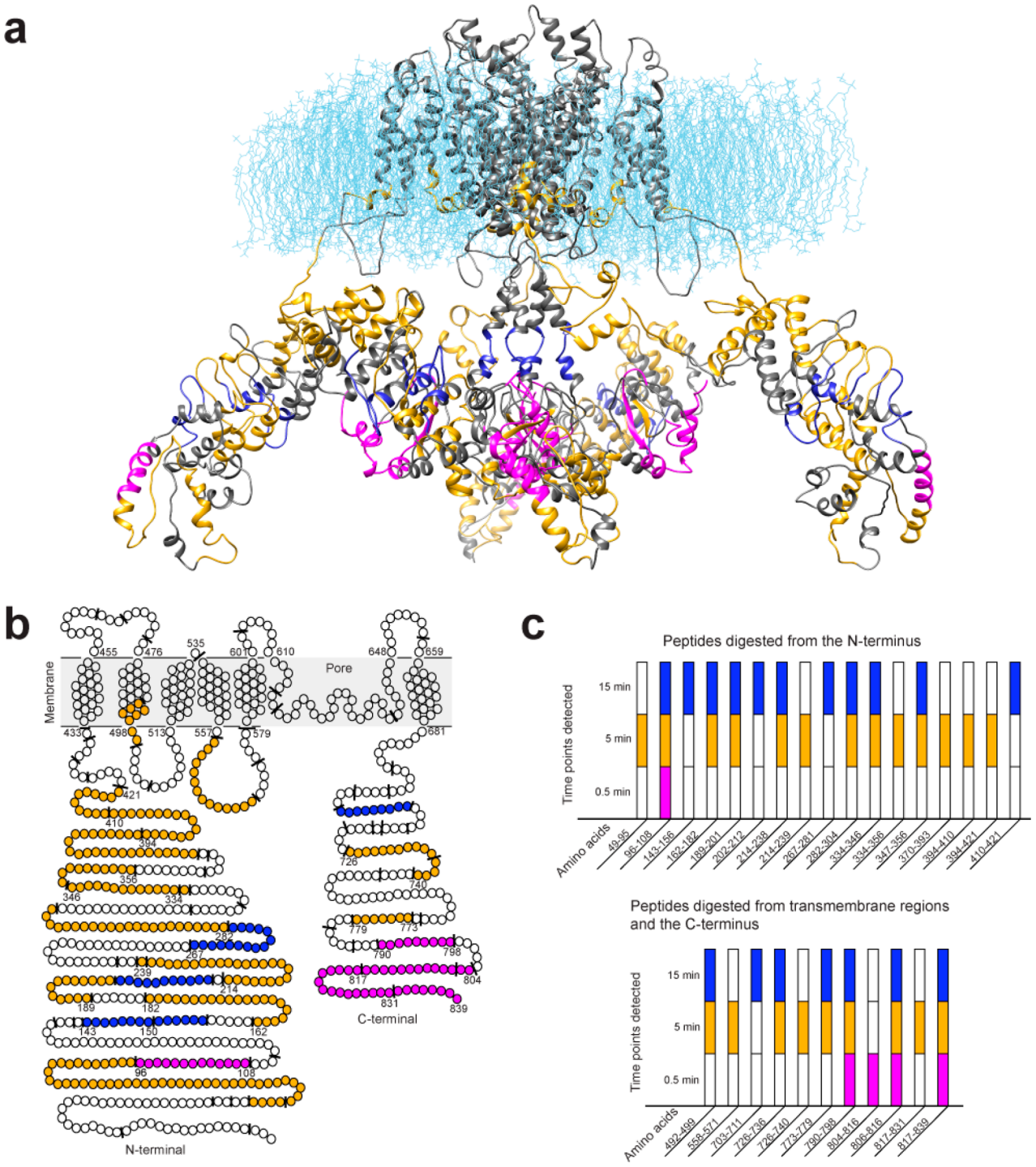

Figure 2. Peptides detected from TRPV1 after limited proteolysis with 5 μg/mL trypsin at room temperature, n = 6. (a) Location of detected peptides shown in a 3D model of TRPV1.[27] Peptides were detected after 0.5 min (magenta), 5 min (orange), and 15 min (blue). (b) Location of detected peptides shown in a schematic representation of TRPV1. Peptides were detected after 0.5 min (magenta), 5 min (orange), and 15 min (blue). Digestion sites are shown when trypsin cleavage probability is >80%. TRPV1 sequence and region information obtained for TRPV1_HUMAN from UniprotKB (www.uniprot.org, accession number Q8NER1) Additional figures showing each single peptide location within the schematic as well as the 3D version of TRPV1 can be found in the Supporting Information (Figures S-2−S-17). (c) Bar plot of detected peptides digested from TRPV1 after limited proteolysis with 5 μg/mL trypsin, showing the time points at which they were confirmed.

20273 sequences, TrEMBL 114605 sequences). Thermo Proteome Discoverer v. 1.3 (Thermo Scientific) was used to validate MS/MS-based peptide and protein identifications.

Electrophysiology with Trypsinization. Inside-out recordings were performed using a microfluidic device for patch-clamp recordings (Dynaflow, Cellectricon AB, Göteborg, Sweden) together with a HEKA EPC10 (Heka Elektronik, Lambrecht, Germany) patch-clamp amplifier. Bath and pipet solutions contained buffers D and E. The patches were clamped at +60 mV, and the current signals were recorded with a sampling frequency of 20 kHz and low-pass-filtered at 5 kHz. Current amplitudes were measured by exposing patches containing several ion channels to 1 μM capsaicin in buffer F during 1 min, followed by a 5 min treatment with either buffer G, 5, 20, or 40 μg/mL trypsin dissolved in buffer G, and finally 1 min of 1 μM

dx.doi.org/10.1021/ja507285w | J. Am. Chem. Soc. 2014, 136, 14875−14882

capsaicin in buffer F. Reversal potentials were measured by using voltage ramp protocols executed at a rate of 1 Hz, with +60 mV as resting potential and ranging from +120 to −30 mV over 150 ms. Ramp protocols were executed during activation with 1 μM capsaicin in buffer F before and after a 5 min treatment with either buffer G, 20, or 40 μg/mL trypsin dissolved in buffer G. EC_{50} values were determined by exposing patches to increasing capsaicin concentrations for 20 s each, using 5 nM, 50 nM, 500 nM, 5 μM, and 50 μM capsaicin in buffer F. The concentration range was applied before and after a 5 min treatment with either buffer G, 20, or 40 μg/mL trypsin dissolved in buffer G. Measurements that shifted largely in seal resistance after treatment were excluded from further analysis.

Data Analysis Electrophysiology. For all measurements, activity after trypsinization was compared to activity after exposure to only buffer in order to exclude any effects of desensitization or potentiation resulting from recurring activations. For data containing current traces, current−time integrated areas were calculated using Fitmaster (HEKA Elektronik) and Matlab (Mathworks, Natick, MA, USA) for each activation with capsaicin between application and 10 s after capsaicin removal. The ratios between the integrated areas for the second and first currents were calculated and compared between treatments. Reversal potentials were calculated using Patchmaster (HEKA Elektronik). EC_{50} values were calculated using GraphPad Prism (GraphPad Software, La Jolla, CA, USA). Spectral analysis of the current traces generated from the experiments was performed using Fitmaster, and ion channel conductance properties were calculated using the following equation:

$$\gamma = \sigma^2/[(E - E_r)I_m(1 - P_o)] \quad (1)$$

where γ is the single-channel conductance, σ^2 is the current variance obtained from the spectral analysis, I_m is the mean current, E is the holding potential, E_r is the reversal potential, and P_o is the probability of channels being open, which is estimated from a concentration−response curve and the EC_{50} value for a specific compound. Statistical analysis was performed with one-way analysis of variance (ANOVA) in combination with Dunnett's post-hoc test, and $p < 0.05$ was considered as statistically significant. Data are presented as mean ± 1 standard deviation.

RESULTS

Probing Surface Topography with LC-MS/MS. An important step when developing pharmaceuticals targeted toward ion channels is to find ligand binding sites within the protein. Identification of surface residues within the tertiary protein structure is an important parameter when predicting binding sites.[21] A possible method for screening surface topology is to restrict the activity of a protease to digest only the most flexible and surface-exposed parts of the protein, by performing limited and controlled proteolysis. Specifically, by controlling the activity of a protease using, e.g., low temperatures, low concentrations, and/or short digestion times, this limited proteolysis technology probes for three main structural determinants: flexible regions that can unfold locally and accommodate the protease, surface-exposed regions, and regions that contain few local interactions, such as hydrogen bonds and disulfide bridges.[22−24] The LPI flow cell provides a means of performing such a kinetically controlled digestion of a membrane protein while avoiding dilution of the sample and maintaining the protein in membrane-derived proteoliposomes, in order to avoid denaturation.

We performed such screening of TRPV1 surface topography using cultured Chinese hamster ovary (CHO) cells expressing human TRPV1, since an expression system was necessary to achieve sufficient material for analysis. TRPV1 consists of four monomers, and each of the monomers has six transmembrane regions, with the ion channel pore region constituted by a tetrameric arrangement of the fifth and the sixth transmembrane domains. A detailed crystal structure is not available for the full-length protein, but the ankyrin repeat domain (ARD) of the N-terminus has successfully been crystallized for rat TRPV1.[25] The 3D structure of TRPV1 has been modeled on the basis of homology with the Kv1.2 channel[26,27] and has been experimentally determined at 19 Å resolution,[28] as well as 3.4 Å resolution,[29] with electron cryomicroscopy. The N- and C-termini of TRPV1 are located on the cytosolic side of the cell membrane and contain several regulatory regions believed to be involved in desensitization, sensitization, and heat activation of the channel.[10,11,25,30,31] Both the N- and C-termini would likely hold several surface-exposed regions due to the regulatory nature of these regions. Proteoliposomes containing TRPV1 were formed from CHO cells and further exposed to limited trypsin proteolysis within the LPI flow cell. The activity of trypsin was controlled by using different digestion times at room temperature. A sequential protocol was used with cumulative incubation times of 0.5, 5, 15, 30, 60, and 120 min, and the digested peptides were detected with liquid chromatography and tandem mass spectrometry (LC-MS/MS) (Figure 2; Supporting Information, Tables S-1−S-7). After 15 min of digestion, the reaction was completed, and no additional peptides were detected. Five peptides were detected after 0.5 min of tryptic digestion, indicating that these regions are very flexible and easily can accommodate the local unfolding which is necessary for trypsin to be able to cut the peptide bonds. The C-terminus has previously been shown to contain an interaction site for calmodulin in the region between aa767 and aa801, where amino acid residues 769, 771, 785, 788, and 797 are essential for binding.[30,32] A peptide that is part of this site, aa790−aa798, containing one of the essential residues, aa797, is detected after 0.5 min of digestion. Eighteen additional peptides were detected after 5 min, a majority of them located in the N-terminus. Peptides located very close to the membrane and toward the end of the N-terminus were digested within this time frame, indicating that the entire N-terminal is very flexible. Suggested ligand interaction sites correlating with the digested peptides from this time point are calmodulin at aa189−aa222,[31] phosphatidylinositol-4,5-bisphosphate (PIP2) at aa189−aa221, and aa778[33] and ATP at aa178 and aa735[34] but also at aa155, aa160, aa199, and aa202.[25] Finally, five peptides were digested after 15 min. Because of the number of hydrogen bonds that would need to be disrupted, digestion is less likely to occur in the middle of an α-helix, which is the location of aa266, and a possible reason why peptide aa267−aa282 was detected late. Peptides may also be located in a crowded region of the protein, which could hinder the activity of the protease.

TRPV1 Activity in Proteoliposomes. The functionality of purified TRPV1 located in liposomes has previously been determined.[28] Here we adapted the same principle in order to test the activity of the channel after removal of different structural segments with tryptic digestion. The activity of TRPV1 was tested by measuring capsaicin-induced calcium release from proteoliposomes loaded with 5 mM Ca^{2+}. Further, calcium-loaded proteoliposomes were immobilized inside the flow cell and subjected to tryptic digestions for 0.5 and 5 min as described above. External calcium concentration was decreased to nanomolar levels (<10 nM) with the use of EGTA, and samples from the external solution were collected before and after TRPV1 activation. Subsequently, calcium release was determined with the fluorescent calcium-binding probe Fura-2

to assess TRPV1 activity in trypsinized and naïve proteoliposomes. The calcium concentration was measured before and after proteoliposome superfusion with capsaicin for 5 min for the trypsinized and naïve ion channels, respectively (Table 1). A significant increase in calcium concentration was observed

Table 1. TRPV1 Activity as a Function of Tryptic Digestion

treatment	calcium concn (nm)
naïve (n = 5)	
control	19.6 ± 3.3
capsaicin	32.2 ± 4.7
tryptic digestion for 0.5 min (n = 10)	
control	20.0 ± 6.1
capsaicin	28.7 ± 10.1
tryptic digestion for 5 min (n = 5)	
control	26.7 ± 11.2
capsaicin	27.6 ± 4.1

both for naïve ion channels and for ion channels treated with trypsin for 0.5 min ($p < 0.05$), whereas a tryptic digestion for 5 min completely inhibited TRPV1 response, as no significant increase of calcium concentration was observed.

Electrophysiology after Trypsinization. Patch-clamp recordings provide detailed functional information about activated ion channels, including ligand-induced modulation of, e.g., their current amplitudes, single-channel conductance, and ion-permeability properties. The inside-out patch-clamp recording configuration was used, allowing the intracellular part of TRPV1 to be exposed to trypsin. Indeed, an outside-out patch-clamp recording configuration could be used in a similar way if the region of interest, e.g., a ligand-binding site, is located on the extracellular side of the ion channel. Changes in functional-related parameters of TRPV1, i.e., current amplitude, reversal potential, EC_{50} value, and single-channel conductance, were determined. The time course of each experiment was kept to a minimum by using different trypsin concentrations instead of altering digestion time. In order to perform a stable inside-out patch-clamp recording, digestions were done in physiological buffers, which slightly altered the digestion pattern compared to the digestions shown in Figure 1a. Here, a 5 min digestion with 5 μg/mL trypsin in physiological buffer (Figure 3a) was determined to yield slightly less peptides than the previously used 0.5 min digestion with a concentration of 5 μg/mL of this enzyme. This was confirmed by performing the digestions with 5 μg/mL trypsin, as well as with 20 and 40 μg/mL trypsin using physiological buffer within the LPI flow cell (Figure 3a–c, Supporting Information, Tables S-8–S-13). By combining patch-clamp recording and flow-cell digestions for proteomic analysis, the effects of chemical truncation of an ion channel can be assessed.

The effect of peptide deletion on ion channel activity can readily be correlated to the observed digestion patterns utilizing the LPI flow cell. During patch-clamp recordings, studying current response, TRPV1 was activated for 1 min with capsaicin and then exposed to trypsin or buffer for 5 min, followed by activation with capsaicin again. The concentration of trypsin was varied between 5, 20, and 40 μg/mL in order to achieve different digestion patterns. Ion channel activation was observed for membrane patches superfused with either buffer or trypsin, but with a decrease in current response with increasing trypsin concentration (Figure 3d). The effects of 5, 20, or 40 μg/mL trypsin treatment on the TRPV1-mediated currents were compared to the control currents by using the current–time integrated areas of the recorded traces. No significant difference between the groups subjected to buffer or 5 μg/mL trypsin were observed, whereas a significant decrease in activity was achieved with 20 and 40 μg/mL trypsin (Figure 4a).

We further investigated the effects of digestions with 20 or 40 μg/mL trypsin on other channel properties; i.e., reversal potentials and EC_{50} values were measured, which indicate changes in the ion permeability as well as the affinity of capsaicin to TRPV1. These functional changes are, thus, related to the structural changes demonstrated in Figure 3a–c, after trypsinization at different concentrations. Superfusion of excised membrane patches with trypsin had no effect on the reversal potential (Figure 4b), whereas a significant increase in EC_{50} values was observed after superfusion with 20 and 40 μg/mL trypsin (Figure 4c). Spectral analysis of the current traces generated from the experiments above was then performed, and ion channel conductance properties were calculated for digestion with 20 and 40 μg/mL trypsin. These calculations revealed a significant decrease in TRPV1 conductance after trypsinization (Figure 4d). Thus, digestion of TRPV1 with 20 and 40 μg/mL trypsin during inside-out patch-clamp recording revealed a decrease in current response by 40% and 55%, a decrease in ion channel conductance by 60% and 70%, and a lower sensitivity toward capsaicin with a 3- and 4-fold increase in EC_{50} values, respectively.

According to eq 1, our data suggest that the decrease in single-channel conductance of the TRPV1 treated with 20 or 40 μg/mL trypsin is the result of a decrease in mean current and increase in EC_{50} values for capsaicin activation of the channel, since the reversal potentials are not affected by the enzyme treatment. Hence, we believe that the peptides cleaved off from TRPV1 after 5 min of exposure to 20 μg/mL trypsin contribute to the decrease of TRPV1 sensitivity toward capsaicin, either by directly altering binding of the agonist or by modulation of any of the regulatory regions within the N- and C-termini of TRPV1.

DISCUSSION

Studying the sequence determinants and structural features that control functionality in ion channels not only expands our understanding of the structures of these channels but also has implications for the development of therapeutic strategies for diseases associated with ion channel dysfunction. Novel method approaches are desired to improve studies of structure–function aspects in ion channels. Here, we perform such studies using a microfluidic approach. We demonstrate that the ion channel TRPV1 can be exposed to limited and controlled trypsin proteolysis in two different microfluidic flow cells under identical experimental conditions. In one instance, patch-clamp recording was performed for pharmacological studies, which gave information on channel function dynamics in an open-volume microfluidic device. This design allows the patch-clamp pipet and cell patch to gain access to the superfusion channels. In another instance, a closed-volume equivalent flow cell was used to digest off peptides from the ion channel without causing dilution of the sample. The cleaved-off peptides were identified with LC-MS/MS. The data from the two experiments were then compared, and the structure–function relationship could be evaluated. Using this methodological approach, we have identified highly flexible regions of TRPV1 as well as key regions that affect functional channel

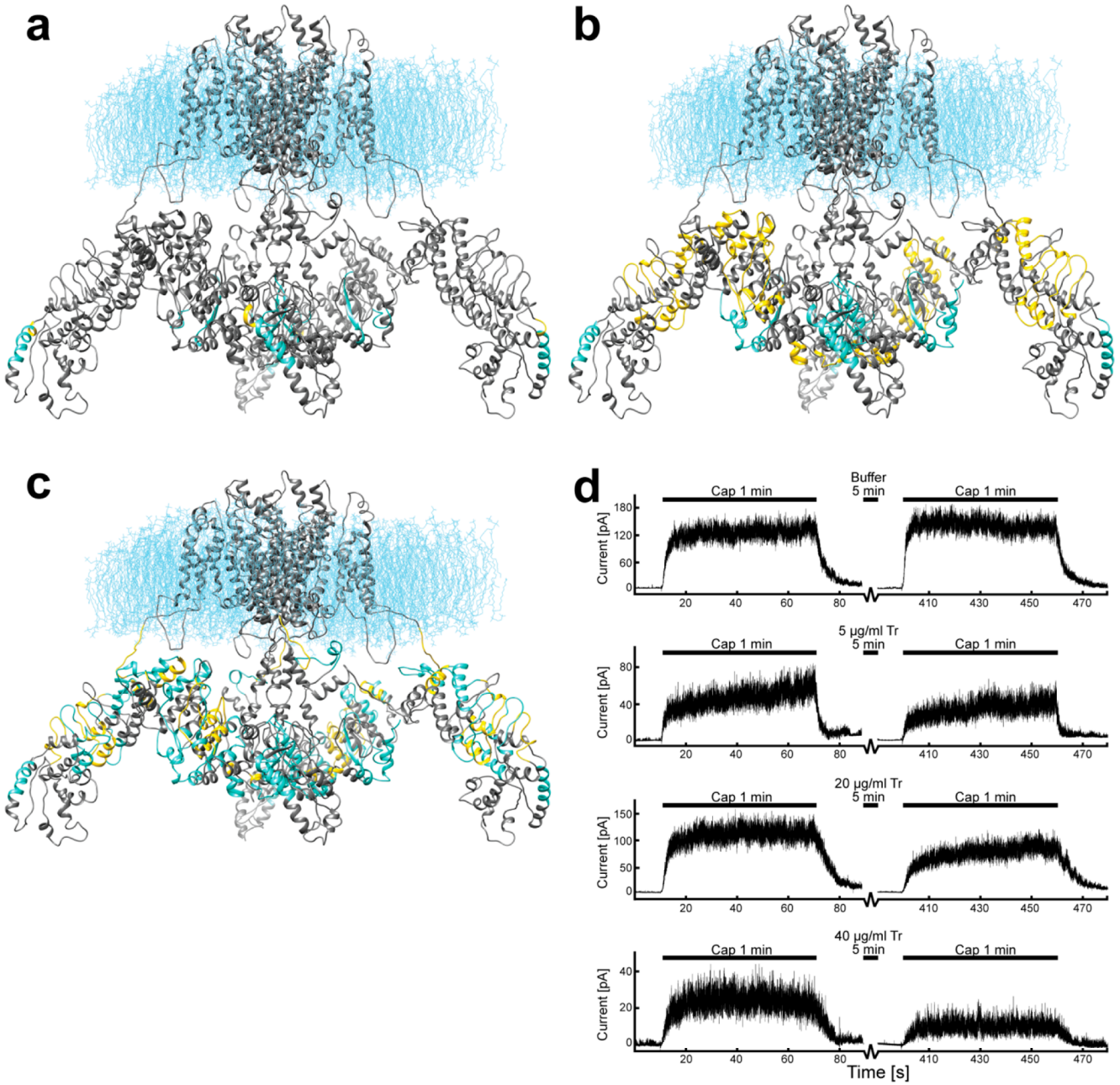

Figure 3. Peptides digested from TRPV1 after 5 min exposure to 5, 20, or 40 μg/mL trypsin (Tr) and the change in current response after their removal. (a–c) Location of digested peptides from TRPV1, showing peptides digested within the flow cell (cyan) and peptides digested within the flow cell followed by a complete digestion overnight (yellow). Schematic representations of the structures shown in panels a–c can be found in the Supporting Information (Figure S-2). (d) Representative traces of inside-out recordings of TRPV1 when activated with 1 μM capsaicin (Cap), followed by 5 min exposure to either buffer or trypsin and an additional activation with capsaicin. From top to bottom: 5 min exposure to buffer and 5, 20, and 40 μg/mL trypsin, respectively. Traces have been digitally filtered at 100 Hz for figure presentation purposes only.

properties during activation with its agonist capsaicin. Several of the regions that were observed with LC-MS/MS as cleaved-off peptides (Figure 2) after limited proteolysis of TRPV1 in the LPI flow cell correlate with known interaction sites for calmodulin, ATP, and PIP2. These results indicate that our microfluidic approach possesses a resolution which enables functional studies of specific interaction sites, or evaluation of putative binding sites for novel ligands or drugs, for a target membrane protein residing in its native lipid environment. The analysis of the results from the capsaicin-induced activation of TRPV1 in the patch-clamp experiment confirmed the capabilities of fine-tuned specificity in this methodological approach for studying structure–function relationships of ion channels. A decrease in single-channel conductance of TRPV1 was achieved (Figure 4d) by increasing the concentration of trypsin from 5 to 20 μg/mL, which resulted in cleavage of additional peptides on the N- and C-termini of TRPV1. Indeed, the binding site of capsaicin to TRPV1 has previously been shown to be associated with the amino acid sequences close to the membrane regions of the protein. However, our and previous studies[10,35] show that capsaicin-induced activation of TRPV1 is reduced when the N- and C-termini are modified. Thus, the peptides cleaved by 5 min exposure of TRPV1 to 20 μg/mL trypsin (Figure 3b) contribute to the decrease in

dx.doi.org/10.1021/ja507285w | J. Am. Chem. Soc. 2014, 136, 14875–14882

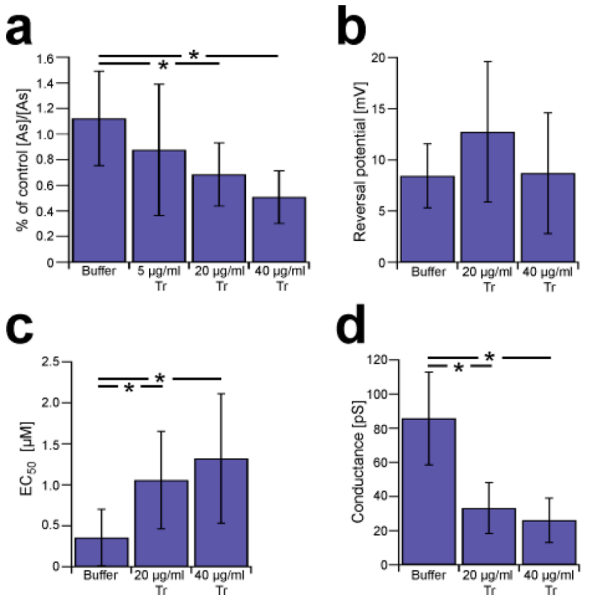

Figure 4. Electrophysiological patch-clamp recordings of TRPV1 function after limited proteolysis with trypsin (Tr). (a) The current trace time-integral for the second activation with capsaicin, calculated as a percentage of the integral for the first activation with capsaicin after treatment with buffer or 5, 20, or 40 μg/mL trypsin, n = 9. (b) Reversal potential for the second activation with capsaicin after treatment with either buffer or 20 or 40 μg/mL trypsin, n = 6. (c) EC_{50} values for the second activation with capsaicin after treatment with either buffer (n = 8) or 20 (n = 8) or 40 μg/mL trypsin (n = 6). (d) Calculated conductance for the second activation with capsaicin after treatment with either buffer or 20 or 40 μg/mL trypsin, n = 9. *Statistical significance calculated with a one-way ANOVA ($p > 0.05$). Data are presented as mean ± 1 standard deviation.

channel activity toward capsaicin, either by directly altering binding of the agonist or by modulating any of the regulatory regions within the N- and C-termini of TRPV1. The use of other enzymes in the demonstrated experimental strategy may also contribute to reveal further binding specificities for ligands (e.g., capsaicin) to the TRPV1 channel.

CONCLUSIONS

We have shown here that limited proteolysis in the LPI flow cell provides a method for screening possible binding sites within functional ion channels residing in membrane-derived proteoliposomes or excised patches. Generally, we have provided a fast and effective method for chemical truncation of a membrane protein, which allows for functional assessment of various peptide regions in the TRPV1 protein. The method can be applied to practically any kind of ion channels and can be extended to additional enzymes having varying site specificity; it can be used in pharmacological protocols for effective screening of novel drugs targeting ion channels.

ASSOCIATED CONTENT

Supporting Information

Additional figures for each peptide and tables of identified peptides. This material is available free of charge via the Internet at http://pubs.acs.org.

AUTHOR INFORMATION

Corresponding Author

owe.orwar@ki.se

Present Addresses

‡E.T.J.: Department of Chemistry and the Beckman Institute for Advanced Science and Technology, University of Illinois at Urbana−Champaign, Urbana, IL 61801, U.S.A.

§K.J.: Department of Physiology and Pharmacology, Karolinska Institutet, SE-171 77 Stockholm, Sweden.

Notes

The authors declare no competing financial interest.

ACKNOWLEDGMENTS

This work was supported by the Knut and Alice Wallenberg Foundation, the European Research Council (ERC) through an advanced ERC Grant, and the Swedish Foundation for Strategic Research (SSF). We thank Dr. Gregorio Fernández-Ballester at the Instituto de Biología Molecular y Celular, Universidad Miguel Hernández, Spain, for kindly letting us use the TRPV1 model. We thank the staff at the Proteomic Core Facility at University of Gothenburg for valuable discussions and comments on the manuscript.

REFERENCES

(1) Ashcroft, F. M. *Nature* **2006**, *440*, 440−447.
(2) Hübner, C. A.; Jentsch, T. J. *Hum. Mol. Genet.* **2002**, *11*, 2435−2445.
(3) Bill, R. M.; Henderson, P. J. F.; Iwata, S.; Kunji, E. R. S.; Michel, H.; Neutze, R.; Newstead, S.; Poolman, B.; Tate, C. G.; Vogel, H. *Nat. Biotechnol.* **2011**, *29*, 335−340.
(4) Carpenter, E. P.; Beis, K.; Cameron, A. D.; Iwata, S. *Curr. Opin. Struct. Biol.* **2008**, *18*, 581−586.
(5) Doyle, D. A.; Morais Cabral, J.; Pfuetzner, R. A.; Kuo, A.; Gulbis, J. M.; Cohen, S. L.; Chait, B. T.; MacKinnon, R. *Science* **1998**, *280*, 69−77.
(6) Yang, W.; Jiang, L.-H. *Methods Mol. Biol.* **2013**, *998*, 257−266.
(7) Reuveny, E.; Slesinger, P. A.; Inglese, J.; Morales, J. M.; Iñiguez-Lluhi, J. A.; Lefkowitz, R. J.; Bourne, H. R.; Jan, Y. N.; Jan, L. Y. *Nature* **1994**, *370*, 143−146.
(8) Jordt, S.-E.; Tominaga, M.; Julius, D. *Proc. Natl. Acad. Sci. U.S.A.* **2000**, *97*, 8134−8139.
(9) Jordt, S.-E.; Julius, D. *Cell* **2002**, *108*, 421−430.
(10) Vlachová, V.; Teisinger, J.; Susánková, K.; Lyfenko, A.; Ettrich, R.; Vyklický, L. *J. Neurosci.* **2003**, *23*, 1340−1350.
(11) Brauchi, S.; Orta, G.; Salazar, M.; Rosenmann, E.; Latorre, R. *J. Neurosci.* **2006**, *26*, 4835−4840.
(12) Hu, H.; Bandell, M.; Grandl, J.; Petrus, M. In *TRP Channels*; Zhu, M. X., Ed.; CRC Press: Boca Raton, 2011; pp 225−272.
(13) Jansson, E. T.; Trkulja, C. L.; Olofsson, J.; Millingen, M.; Wikström, J.; Jesorka, A.; Karlsson, A.; Karlsson, R.; Davidson, M.; Orwar, O. *Anal. Chem.* **2012**, *84*, 5582−5588.
(14) Bruus, H. *Theoretical Microfluidics*; Oxford University Press: Oxford, 2007.
(15) Caterina, M. J.; Schumacher, M. A.; Tominaga, M.; Rosen, T. A.; Levine, J. D.; Julius, D. *Nature* **1997**, *389*, 816−824.
(16) Tominaga, M.; Caterina, M. J.; Malmberg, A. B.; Rosen, T. A.; Gilbert, H.; Skinner, K.; Raumann, B. E.; Basbaum, A. I.; Julius, D. *Neuron* **1998**, *21*, 531−543.
(17) Levine, J. D.; Alessandri-Haber, N. *Biochim. Biophys. Acta* **2007**, *1772*, 989−1003.
(18) Gunthorpe, M. J.; Chizh, B. A. *Drug Discovery Today* **2009**, *14*, 56−67.
(19) Palazzo, E.; Luongo, L.; De Novellis, V.; Rossi, F.; Marabese, I.; Maione, S. *Curr. Opin. Pharmacol.* **2012**, *12*, 9−17.
(20) Jansson, E. T.; Trkulja, C. L.; Ahemaiti, A.; Millingen, M.; Jeffries, G. D.; Jardemark, K.; Orwar, O. *Mol. Pain* **2013**, *9*, 1.
(21) Khazanov, N. A.; Carlson, H. A. *PLoS Comput. Biol.* **2013**, *9*, No. e1003321.
(22) Hubbard, S. J.; Beynon, R. J.; Thornton, J. M. *Protein Eng.* **1998**, *11*, 349−359.

(23) Hubbard, S. J. *Biochim. Biophys. Acta* **1998**, *1382*, 191−206.
(24) Fontana, A.; De Laureto, P. P.; Spolaore, B.; Frare, E.; Picotti, P.; Zambonin, M. *Acta Biochim. Polym.* **2004**, *51*, 299−321.
(25) Lishko, P. V.; Procko, E.; Jin, X.; Phelps, C. B.; Gaudet, R. *Neuron* **2007**, *54*, 905−918.
(26) Brauchi, S.; Orta, G.; Mascayano, C.; Salazar, M.; Raddatz, N.; Urbina, H.; Rosenmann, E.; Gonzalez-Nilo, F.; Latorre, R. *Proc. Natl. Acad. Sci. U.S.A.* **2007**, *104*, 10246−10251.
(27) Fernández-Ballester, G.; Ferrer-Montiel, A. *J. Membr. Biol.* **2008**, *223*, 161−172.
(28) Moiseenkova-Bell, V. Y.; Stanciu, L. A.; Serysheva, I. I.; Tobe, B. J.; Wensel, T. G. *Proc. Natl. Acad. Sci. U.S.A.* **2008**, *105*, 7451−7455.
(29) Liao, M.; Cao, E.; Julius, D.; Cheng, Y. *Nature* **2013**, *504*, 107−112.
(30) Numazaki, M.; Tominaga, T.; Takeuchi, K.; Murayama, N.; Toyooka, H.; Tominaga, M. *Proc. Natl. Acad. Sci. U.S.A.* **2003**, *100*, 8002−8006.
(31) Rosenbaum, T.; Gordon-Shaag, A.; Munari, M.; Gordon, S. E. *J. Gen. Physiol.* **2004**, *123*, 53−62.
(32) Grycova, L.; Lansky, Z.; Friedlova, E.; Obsilova, V.; Janouskova, H.; Obsil, T.; Teisinger, J. *Biochem. Biophys. Res. Commun.* **2008**, *375*, 680−683.
(33) Grycova, L.; Holendova, B.; Bumba, L.; Bily, J.; Jirku, M.; Lansky, Z.; Teisinger, J. *PLoS One* **2012**, *7*, No. e48437.
(34) Kwak, J.; Wang, M. H.; Hwang, S. W.; Kim, T. Y.; Lee, S. Y.; Oh, U. *J. Neurosci.* **2000**, *20*, 8298−8304.
(35) Jung, J.; Lee, S.-Y.; Hwang, S. W.; Cho, H.; Shin, J.; Kang, Y.-S.; Kim, S.; Oh, U. *J. Biol. Chem.* **2002**, *277*, 44448−44454.